THE RECIPROCAL APPROACH TO THE INVERSE PROBLEM OF ELECTROENCEPHALOGRAPHY

Stefan Finke[1], Ramesh M. Gulrajani[1], Jean Gotman[2]

[1]Institute of Biomedical Engineering, Université de Montréal, Montréal, Québec, Canada
[2]Montreal Neurological Institute, McGill University, Montréal, Québec, Canada

Abstract - **Forward transfer matrices relating dipole source to surface potentials can be determined via conventional or reciprocal approaches. In numerical simulations with a triangulated boundary-element three-concentric-spheres head model, we compare four inverse EEG solutions: those obtained with conventional and reciprocal transfer matrices, and relating in each case dipole components to potentials at either triangle centroids or triangle vertices. Dipole localization errors are presented in all four cases for varying dipole eccentricity and two different values of skull conductivity. For tangential dipoles, the reciprocal vertex approach performed best overall when considering both skull conductivities. No such clear-cut conclusion could be drawn for radial dipoles.**
Keywords - **Electroencephalography, dipole source localization, boundary element method, inverse problem, reciprocity**

I. INTRODUCTION

There has been much recent interest in a reciprocal approach to the inverse problem of electroencephalography (EEG), whereby the forward transfer matrix relating dipole source to the generated potentials at the surface electrode sites is obtained via a reciprocal approach. The reciprocal approach entails calculating the electric field that results at the dipole location from current injection and withdrawal at the surface electrode sites [1]. The forward transfer coefficients are then obtained from a scalar product of this electric field with the source dipole. The major advantage of such a reciprocally-computed transfer matrix is that the volume conductor geometry can be refined exclusively at the known surface-electrode positions, presumably increasing the precision of the transfer matrix, and hence that of the computed inverse dipole. Recent examples of inverse solutions obtained with reciprocally-computed transfer matrices have been published, based on finite-difference [2] and finite-element [3] volume conductor discretizations. We describe herein some preliminary simulation studies of the accuracy of such inverse solutions, but employing a boundary-element volume conductor discretization instead. Furthermore, recent evidence [4] suggests that the skull conductivity may be much higher than previously assumed, and that this has important ramifications for the forward problem [5]. The effect of this higher skull conductivity on inverse EEG solutions is also considered.

II. METHODOLOGY

A. Conventional approach

Assuming that a neural source can be represented by a current dipole $\mathbf{J}_s$ at a given location in the brain volume conductor, the potential difference between any two given scalp electrodes A and B may be expressed as

$$u_{AB} = \mathbf{L} \cdot \mathbf{J}_s \tag{1}$$

where $\mathbf{L}$ is a so-called "lead vector". The lead vector may be obtained by calculating the potentials u_{AB} corresponding to unit dipoles in the x, y, and z directions at the dipole location under consideration. Assigning the three potential values determined in this way to the individual lead vector components L_x, L_y, and L_z, respectively, corresponds to the conventional approach to the forward problem of electroencephalography. For accurate computations, however, the low conductivity of the skull mandates the use of a two-step "isolated-problem" implementation [6] whereby potentials are first computed assuming a skull of zero conductivity following which, in a second computation, these "isolated" potentials are corrected for the real skull conductivity. Also, a simple matrix deflation technique [7] is needed in these potential computations to counter the singular matrix that results on account of the indeterminacy of the potential to within a constant.

B. Reciprocal approach

An alternative determination of $\mathbf{L}$ invokes Helmholtz' principle of reciprocity which states that $\mathbf{L} = -\mathbf{E}$, where $\mathbf{E}$ is the electric field or "lead field" at the dipole location resulting from a unit current injected into the volume conductor at electrode A and withdrawn at electrode B. The reciprocal approach to the forward problem thus entails first calculating $\mathbf{E}$ in a volume conductor which is now assumed passive (containing no dipole sources), and then the potential u_{AB} which is given by $u_{AB} = -\mathbf{E} \cdot \mathbf{J}_s$. Matrix deflation is also needed in the reciprocal approach when computing $\mathbf{E}$.

C. Inverse solution

Next, let $\mathbf{U}$ be the $N \times 1$ column matrix containing the potential differences between the N surface electrode pairs on the scalp. For a particular *fixed* trial dipole location, $\mathbf{T}$ is defined as the $N \times 3$ transfer matrix containing the three individual lead vector components L_x, L_y, and L_z for each of the N electrode pairs considered. From (1), the theoretical potentials $\mathbf{U}$ can be calculated via the matrix relation $\mathbf{U} = \mathbf{T}\mathbf{J}_s$. Given a measured potential distribution (with reference potential subtracted) characterized by the $N \times 1$ column matrix $\hat{\mathbf{U}}$, the "best" dipole moment at this particular dipole location can be estimated from a standard linear least-squares minimization of the sum-squared residual $R = (\hat{\mathbf{U}} - \mathbf{U})^T(\hat{\mathbf{U}} - \mathbf{U})$, where T denotes the transpose. The best moment of this trial dipole is given by the so-called "normal equations" [8]

$$\mathbf{J}_s = \mathbf{T}^+\hat{\mathbf{U}} \tag{2}$$

where $\mathbf{T}^+ = (\mathbf{T}^T\mathbf{T})^{-1}\mathbf{T}^T$ is known as the "Moore-Penrose pseudo-inverse" of the matrix $\mathbf{T}$. Using this value for $\mathbf{J}_s$, the residual R can be written as

$$R = \hat{\mathbf{U}}^T[\mathbf{I} - \mathbf{T}\mathbf{T}^+]\hat{\mathbf{U}} \tag{3}$$

Report Documentation Page

Report Date 25 Oct 2001	Report Type N/A	Dates Covered (from... to) -

Title and Subtitle The Reciprocal Approach to the Inverse Problem of Electroencephalography	Contract Number
	Grant Number
	Program Element Number

Author(s)	Project Number
	Task Number
	Work Unit Number

Performing Organization Name(s) and Address(es) Institute of Biomedical Engineering Universite de Montreal Montreal, Quebec, Canada	Performing Organization Report Number

Sponsoring/Monitoring Agency Name(s) and Address(es) US Army Research, Development & Standardization Group (UK) PSC 802 Box 15 FPO AE 09499-1500	Sponsor/Monitor's Acronym(s)
	Sponsor/Monitor's Report Number(s)

Distribution/Availability Statement
Approved for public release, distribution unlimited

Supplementary Notes
Papers from 23rd Annual International Conference of the IEEE Engineering in Medicine and Biology Society, October 25-28, 2001, held in Istanbul, Turkey. See also ADM001351 for entire conference on cd-rom.

Abstract

Subject Terms

Report Classification unclassified	Classification of this page unclassified

Classification of Abstract unclassified	Limitation of Abstract UU

Number of Pages
4

where **I** is the $N \times N$ identity matrix. The well-known simplex algorithm can now be used to select the best location for the trial dipole by minimizing the above expression for the sum-squared residual [9]. In practice, we did not minimize R but rather the relative-difference error measure (RDM) obtained by first dividing R by the N sum-squared measured potentials in **Û** and then taking the square root. Note that the simplex algorithm only searches for the three location coordinates of the dipole, since the dipole moment is always given by (2).

D. Three-concentric-spheres head models

In order to test the conventional and reciprocal approaches to inverse EEG computations, the well-known three-concentric-spheres head model was employed with two different sets of relative conductivities for the scalp, skull, and cortex: 1, 1/80, 1 and 1, 1/15, 1, respectively. The first set corresponds to the values usually employed for these conductivities, the second reflects the higher skull conductivity suggested by more recent work [4]. Sphere radii were 10 cm, 9.2 cm, and 8.7 cm. Forward potentials were calculated via analytic equations [10] at 41 uniformly distributed electrode sites on the outermost sphere (a 42nd electrode was used as the reference electrode). The spheres were discretized into planar triangles employing regularly-spaced lines of latitude and longitude, except around the 42 electrode sites where a higher triangle density was used (Fig. 1a). With the conventional approach, potentials may be calculated either at triangle centroids or at triangle vertices. With the former, the potential is assumed constant across each triangle, with the latter a linear variation in potential was assumed. In the conventional centroid (CC) approach, the centroid of the innermost triangle in each high-density region coincided with the electrode position. With the conventional vertex (CV) approach, one of the vertices of the innermost triangle was selected as the electrode site. In the reciprocal approach also, potentials may be determined at triangle centroids or vertices. Thus, in the reciprocal centroid approach (RC), the centroids of the innermost triangles were used for reciprocal current injection and withdrawal. A slightly different discretization was used with the reciprocal vertex (RV) approach where a curvilinear quadrilateral innermost element was used, with quadratic interpolation of the potential for this element alone and with the site of current injection at the center of the quadrilateral (Fig. 1b).

Two levels of discretization were used, level 1 employing 1572 and level 2 employing 2228 triangles per sphere. Level 1 was used for the CC and RC approaches, but level 2 was used for the CV and RV approaches. This is because in a triangular discretization the number of vertices is approximately half the number of triangles, and this permits using a finer discretization for the vertex approach while keeping the same number of unknown potentials. Note that for the RV approach, the triangular discretization had to be modified slightly to allow the insertion of a quadrilateral at each electrode site. For this approach, in addition to 42 curvilinear quadrilaterals, a level 1 discretization corresponds to 1866 triangles whereas a level 2 discretization corresponds to 2522 triangles. Only level 1 discretizations are shown in Fig. 1.
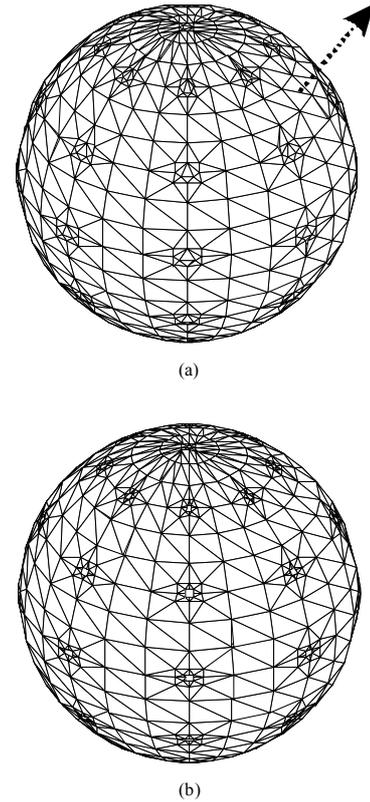

Fig. 1. Level 1 sphere discretizations. There are 1572 triangles per sphere in (a) and 1866 triangles in addition to 42 curvilinear quadrilaterals in (b). CC, CV, and RC approaches use sphere (a) and the RV approach uses sphere (b). The 45° axis along which the dipole is moved is shown dotted in (a).

E. Simplex Minimization

The analytically-computed potentials were perturbed by the addition of 10% Gaussian noise (corresponding to a signal-to-noise ratio of 20 db) at the 42 electrode sites to be used for inverse computations. This noise level was selected as representative of the noise to be expected during EEG measurement. Identical noise-added potentials were used for the CC and RC solutions, and for the CV and RV ones. For each inverse solution, 10 simplex minimizations with different randomly-chosen starting points were run, with stopping points either when the difference in RDM between successive simplex iterations dropped below 0.0001 or following a maximum of 1000 iterations. An individual simplex minimization could return a result of non-convergence (having reached the maximum of 1000 iterations), convergence to the correct known position of the dipole source, or convergence to an incorrect solution. All correctly converging simplexes had RDM measures less than 0.1, except in one instance (see Results). RDM measures for the incorrect solutions were always larger than those for the correct solutions, thereby permitting us to distinguish between incorrect and correct solutions even if the true dipole coordinates were not known. This is important for the eventual application of the simplex technique to real patients. The computed dipole location was obtained from the simplex with the least RDM among the set of correctly converging simplexes. The position error between the starting dipole and
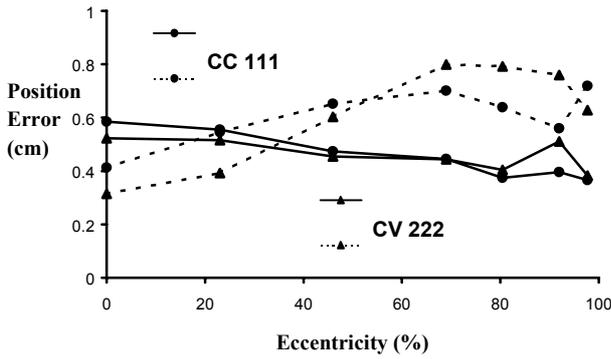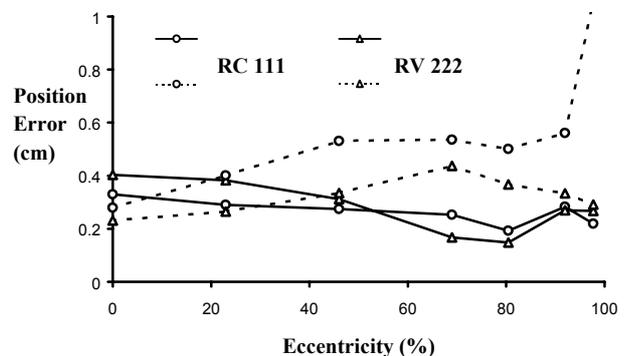
(a)
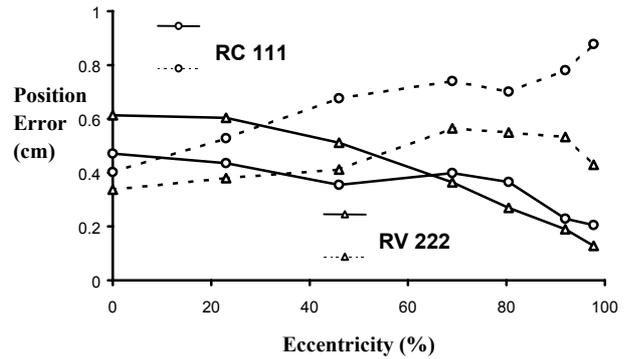
(a)
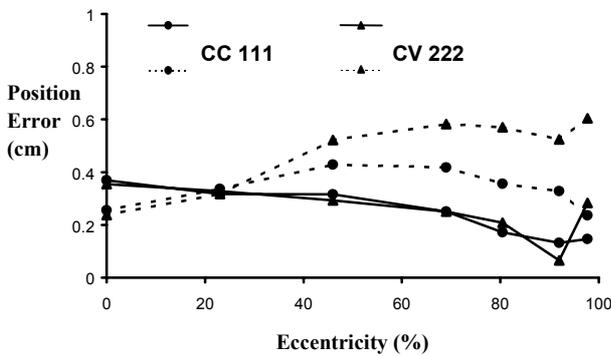
(b)

(b)

Fig. 2. Dipole position error plotted against dipole eccentricity for radial (solid line) and tangential (dotted line) dipoles. Results for both CC (circles) and CV (triangles) approaches are depicted. Relative skull conductivity was 1/80 in (a) and 1/15 in (b).

Fig. 3. Dipole position error plotted against dipole eccentricity for radial (solid line) and tangential (dotted line) dipoles. Results for both RC (circles) and RV (triangles) approaches are depicted. Relative skull conductivity was 1/80 in (a) and 1/15 in (b).

this computed dipole location was used as an index of precision for each of the four approaches.

III. RESULTS

Test simulations were run using radial and tangential source dipoles along a central 45 degree axis (shown dotted in Fig. 1a). Dipole eccentricities ranged from zero to a maximum of 8.5 cm (97.7% of the innermost sphere radius). Graphs of the resulting inverse-dipole position errors at varying eccentricities for CC and CV approaches and for each of the two values of relative skull conductivities considered (σ_{skull} = 1/80 and 1/15) are shown in Fig. 2. Similar graphs for the RC and RV approaches are plotted in Fig. 3. A discretization designated 111 (222) meant that level 1 (2) spheres were used for the three-concentric-spheres model. As already mentioned, a 111 discretization was used for CC and RC approaches and a 222 discretization for CV and RV ones. In general, the position error is greater for tangential dipoles than for radial dipoles for all four approaches. This is especially true for eccentric dipoles. The

position error decreased for all approaches with a relative skull conductivity of 1/15 instead of 1/80 (approximately 3 mm on average instead of 5 mm). For tangential dipoles, the RV approach performed best overall when considering both skull conductivities. No such clear-cut conclusion could be drawn for radial dipoles. A position error greater than 1 cm was only obtained with the RC approach and the most eccentric (97.7%) tangential dipole in a model with relative skull conductivity of 1/15. This is almost certainly related to the assumption of a constant potential across triangle faces. This assumption is especially inadequate at the electrode (current injection) sites. This was also the only case where the RDM increased to 0.13.

The number of correct, incorrect, and non-convergent simplex solutions for each approach and for each of the two values of relative skull conductivity is shown in Table I. Note that with the RC approach, for a tangential dipole at an eccentricity of 97.7% and both sets of conductivities, most of the 10 simplex algorithms did not converge within 1000 iterations. The lower percentage of correct simplex solutions for the RC option when compared to the other options in Table I is largely due to this fact.

IV. Discussion

In an earlier study done by us [5] that focused on the accuracy of the forward transfer coefficients determined by each of the four approaches, it was shown, using the same three-concentric-spheres head models, that RDMs for the forward problem can increase dramatically with high dipole eccentricities. This increase in forward-problem RDMs, however, does not translate to larger position errors for inverse computations with eccentric dipole sources (Figs. 2 and 3), except for the RC approach and a tangential dipole at 97.7% eccentricity where it was attributed to the assumption of a constant potential at the current injection site. One possible reason for reasonable position errors, despite the increased forward-problem RDMs for eccentric dipoles, could be the inclusion of a constraint with the simplex algorithm inhibiting inverse dipole determinations outside the innermost sphere. This constraint is evidently most in use for highly-eccentric dipoles and could serve to compensate for the greater inaccuracy of transfer coefficients for such dipoles. Another reason for acceptable errors with eccentric dipoles could be the added Gaussian noise in the surface potentials which may "wash" out the differences in forward transfer matrix precisions for centric and eccentric dipoles. Whatever the reason, it augurs well for inverse solutions that eccentric source dipoles can be located with reasonable precision.

At the same time, dipole moment and orientation errors do increase greatly for highly-eccentric dipoles, both radial and tangential. Inverse-solution RDM values, however, remained less than 0.1 except for the one case mentioned above of the RC solution for a tangential dipole and a relative skull conductivity of 1/15. Thus, the error in the forward-problem RDM at high eccentricities manifests itself in larger moment and orientation errors at these eccentricities rather than in an increased position error.

V. Conclusion

Both the conventional and reciprocal approaches produced inverse solutions of comparable accuracy, with a slight advantage being noted in these preliminary studies for the RV approach in the case of tangential dipoles. The new higher estimate of the relative skull conductivity results in reduced position error. Finally, in inverse computations with highly-eccentric source dipoles, it was more the moment and orientation error that increased rather than the position error.

Acknowledgments

TABLE I
PERCENTAGE OF CORRECT, INCORRECT, AND NON-CONVERGENT SIMPLEX SOLUTIONS

Approach		Number per category (%)		
		Correct	Incorrect	Non-convergent
CC :				
σ_{skull} =	1/80	93.6	5.7	0.7
	1/15	95.7	4.3	0.0
CV :				
σ_{skull} =	1/80	95.0	5.0	0.0
	1/15	93.6	4.3	2.1
RC :				
σ_{skull} =	1/80	87.1	4.3	8.6
	1/15	85.7	5.0	9.3
RV :				
σ_{skull} =	1/80	90.7	5.0	4.3
	1/15	95.0	2.1	2.9

References

[1] D.J. Fletcher, A. Amir, D.L. Jewett, and G. Fein, "Improved method for computation of potentials in a realistic head shape model," *IEEE Trans. Biomed. Eng.*, vol. 42, pp. 1094-1104, 1995.

[2] P. Laarne, J. Hyttinen, S. Dodel, J. Malmivuo, and H. Eskola, "Accuracy of two dipolar inverse algorithms applying reciprocity for forward calculation," *Comp. Biomed. Res.*, vol. 33, pp. 172-185, 2000.

[3] D. Weinstein, L. Zhukov, and C. Johnson, "Lead-field bases for electroencephalography source imaging," *Ann. Biomed. Eng.*, vol. 28, pp. 1059-1065, 2000.

[4] T.F. Oostendorp, J. Delbeke, and D.F. Stegeman, "The conductivity of the human skull: Results of in vivo and in vitro measurements," *IEEE Trans. Biomed. Eng.*, vol. 47, pp. 1487-1492, 2000.

[5] S. Finke and R.M. Gulrajani, "Conventional and reciprocal approaches to the forward problem of electroencephalography," *Electromagnetics [Special issue on Bioelectromagnetic Forward and Inverse Problems]*, 2001, in press.

[6] M.S. Hamalainen and J. Sarvas, "Realistic conductivity geometry model of the human head for interpretation of neuromagnetic data," *IEEE Trans. Biomed. Eng.*, vol. 36, pp. 165-171, 1989.

[7] M.S. Lynn and W.P. Timlake, "The use of multiple deflations in the numerical solution of singular systems of equations, with applications to potential theory," *SIAM J. Numer. Anal.*, vol. 5, pp. 303-322, 1968.

[8] G.E. Forsythe and C.B. Moler, *Computer Solution of Linear Algebraic Systems*, Englewood Cliffs, NJ: Prentice-Hall, 1967, pp. 16.

[9] B. He, T. Musha, Y. Okamoto, S. Homma, Y. Nakajima, and T. Sato, "Electric dipole tracing in the brain by means of the boundary element method and its accuracy," *IEEE Trans. Biomed. Eng.*, vol. 34, pp. 406-414, 1987.

[10] J. Ary, S. Klein, and D. Fender, "Location of sources of evoked scalp potentials: corrections for skull and scalp thickness," *IEEE Trans. Biomed. Eng.*, vol. 28, pp. 447-452, 1981.